Water Research 83 (2015) 184–194

Contents lists available at ScienceDirect

Water Research

journal homepage: www.elsevier.com/locate/watres

Hydraulic continuity and biological effects of low strength very low frequency electromagnetic waves: Case of microbial biofilm growth in water treatment

Merlin Gérard [a, *], Omri Noamen [a], Gonze Evelyne [a], Valette Eric [b], Cauffet Gilles [c, d], Henry Marc [e]

[a] LOCIE UMR CNRS 5271, Université de Savoie, 73376, Le Bourget du Lac, France
[b] Planet Horizons Technologies, Technopole 5, 3960 Sierre, Switzerland
[c] Univ. Grenoble Alpes, G2Elab, F-38000 Grenoble, France
[d] CNRS, G2Elab, F-38000 Grenoble, France
[e] LCMES UMR CNRS 7140 Université de Stasbourg, 67000 Strasbourg, France

ARTICLE INFO

Article history:
Received 15 September 2014
Received in revised form
6 June 2015
Accepted 25 June 2015
Available online 30 June 2015

Keywords:
Water treatment
Microbial biomass
VLF electromagnetic fields
Quantum field theory
Water coherence

ABSTRACT

This study aims to elucidate the interactions between water, subjected to electromagnetic waves of very low frequency (VLF) (kHz) with low strength electromagnetic fields (3.5 mT inside the coils), and the development of microbial biofilms in this exposed water. Experimental results demonstrate that in water exposed to VLF electromagnetic waves, the biomass of biofilm is limited if hydraulic continuity is achieved between the electromagnetic generator and the biofilm media. The measured amount of the biofilm's biomass is approximately a factor two lower for exposed biofilm than the non-exposed biofilm. Measurements of electromagnetic fields in the air and simulations exhibit very low intensities of fields (<10 nT and 2 V/m) in the biofilm-exposed region at a distance of 1 m from the electromagnetic generator. Exposure to electric and magnetic fields of the quoted intensities cannot explain thermal and ionizing effects on the biofilm. A variable electrical potential with a magnitude close to 20 mV was detected in the tank in hydraulic continuity with the electromagnetic generator. The application of quantum field theory may help to explain the observed effects in this case.

1. Introduction

Although a number of studies have been conducted over many years, the effect of very low frequency (VLF) electric and magnetic fields (EMF) on living organisms is still insufficiently understood, particularly at low intensity. Radio frequencies (RF) in the range of 3 kHz–30 kHz and wavelenghts from 1 to 10 km are considered to be in the VLF regime. A decrease in biofilm has been empirically noted after electromagnetic treatment of limescale formation in water supply lines of poultry farms and irrigation systems using VLF electromagnetic commercial systems. Treatment of seawater with the same electromagnetic system enabled the partial removal of a mature biofilm adhering to the inner surfaces of the tubes of a heat exchanger-condenser (Trueba et al., 2014). Therefore, it is interesting to investigate the effect of VLF-EMF on biofilm formation in water, through a multidisciplinary approach, under controlled conditions.

Generally speaking, biofilms are defined as a complex community of bacteria, fungi, protozoa and macroinvertebrates with several trophic levels as observed for wastewater biofilms (Tsuneda et al., 2003). Biofilm development on a medium is achieved in several steps (O'Toole et al., 2000): initiation, adhesion, growth, maturation, and detachment. Many factors affect the various steps and involve the physicochemical properties of the substrate, biotic factors and/or environmental factors (Mueller, 1996). Organization of microorganisms in biofilm enables optimal use of available substrates and protects the microorganisms from adverse conditions and stress (Jefferson, 2004). Also, 70–90% of the dry mass of biofilms consists of extracellular polymeric substances (Tsuneda et al., 2003) which gives the biofilm the properties of a gel with a highly hydrophilic porous structure containing up to 95% H_2O. Although in certain cases the presence of biofilms is good (e.g.

* Corresponding author.
E-mail address: gerard.merlin@univ-savoie.fr (M. Gérard).

http://dx.doi.org/10.1016/j.watres.2015.06.041
0043-1354/

bioprocesses case), in many cases, this presence can have a negative effect due to clogging or health problems; and various techniques are subsequently used to limit or eradicate the unwanted biofilm (Costerton et al., 1999).

Biological effects due to RF exposure; including VLF waves, are classified as thermal effects and non-thermal effects in lower energy fields. Non-thermal effects of electromagnetic waves are the most difficult to identify due to the low exposure energies. Interaction of EMFs with matter can be modeled from the microscopic level to the macroscopic level (Baker-Jarvis and Sung, 2012). In theory, the electromagnetic field interactions with biological matter may be modeled on a microscopic scale by applying quantum mechanics and by using Maxwell's equations at macroscopic level. It is challenging to model interactions in the mesoscopic scale (10^{-7} m–10^{-4} m) since classical analysis begins to be modified by quantum mechanics. According to the quasi-static nature of EMF at low frequencies, such RF electric and magnetic fields act independently of one another (Habash Riadh, 2006) and bioelectric or biomagnetic phenomena are commonly modeled as quasi-static cases in which electric and magnetic fields can be studied separately (Zhou and Uesaka, 2006). Dielectric response of biological materials is related to membrane and cell boundaries, molecular dipoles, together with associated ionic fluids and counterions (Baker-Jarvis and Sung, 2012). At a molecular level RF-EMF interact with moving charges, similar to electrons in cytochrome oxidase (Blank and Soo, 2001).

To the best of our knowledge excluding the work of Trueba et al. (2014), the only studies published on the effects of EMFs on biofilms concern extremely low frequency EMF. Although VLF electromagnetic waves are slightly more energetic than extremely low frequencies (ELF) electromagnetic waves, the nature of observed non-thermal effects could be similar to ELF electromagnetic waves. For prokaryotic systems, exposure to electromagnetic fields produce effects of stress, causing phenotypic and genetic perturbations of planktonic cells (free cells) that may affect the adhesion of these cells and their organization into a biofilm (Cellini et al., 2008; Chua and Yea, 2005; Del re et al., 2004). Bacterial cultures of *Helicobacter pylori ATCC 43629* were exposed to a low frequency magnetic field (50 Hz, 1 mT intensity) for two days (Di Campli et al., 2010). The magnetic field acted on the bacterial population during the formation of the biofilm and after the maturation phase by decreasing cell viability and cell mass when compared to the control biofilm. Based on the work of Pickering et al. (Pickering et al., 2003) when Staphylococcus epidermidis biofilms aged 5 days and incubated 12 h with various concentrations of antibiotics (vancomycin or gentamicin) at 37 °C and 5% CO_2, are exposed to ELF-EMF (72 Hz), the efficiency of gentamicin against biofilms increases by at least 50%. It was also found that electrical fields with low intensity (1.5–20 V cm^{-1}) and current densities ranging from 15 μA cm^{-2} to 2.1 mA cm^{-2} can decrease the inherent resistance of bacterial biofilms to biocides (Blenkinsopp et al., 1992) and antibiotics (Costerton et al., 1994). This bioelectric effect reduces by a factor 1.5 to 4.0 the required concentrations of these antibacterial agents to kill the biofilm bacteria.

In this study we investigated the formation and development of biofilms on glass slides exposed to water subjected to VLF electromagnetic waves. This study represents only part of the ongoing work to characterize the effects of electromagnetic fields at very low frequencies and low intensities on the growth of microorganisms in aqueous media. This work corresponds to a first approach to verify and quantify empirical observations found *in situ*.

Compared with previous studies done with ELF-EMF, the biofilm in our study was not exposed in the heart of the generator but at a distance of one meter, where the field strengths in the air were extremely weak. Both the presence and lack of hydraulic continuity was investigated to assess its role in the transmission of EMF and their possible effects between the generator and the biofilm on glass supports. The assumption would be that the high sensitivity of liquid water to electromagnetic waves was due to its organization in coherence domains (CD), as calculated with quantum field theory (Bono et al., 2012). Under this assumption liquid water is organized in domains by a stacking of coherence overlapping with each other and holding cold vortices of quasi-free electrons (Marchettini et al., 2010), making it sensitive to electromagnetic fields on the order of a few kHz. Intracellular water maintaining its coherence would also be sensitive to electromagnetic waves of very low frequencies, resulting in a disturbance of the metabolic activities (Del Guidice et al., 2010).

2. Materials and methods

2.1. Experimental device (Fig. 1)

Glass slides were placed in glass tanks fed by a nutrient solution that had previously passed through an electromagnetic wave generator (Aqua-4D 60E Pro® from Planet Technologies Horizons, Switzerland). The use of a synthetic nutrient solution enabled control of the operating conditions, particularly the applied organic load: starch 0.05 g/L; glucose 0.05 g/L; KH_2PO_4 1.25 mg/L; $(NH_4)_2SO_4$ 2.5 mg/L; CH_3CO_2Na 2.5 mg/L; peptones 2.5 mg/L. The chemical oxygen demand (COD) was close to 100 mg/L, the electrical conductivity was 0.36 ± 0.027 mS cm^{-1} and the pH of the nutrient solution was 7.2. These physicochemical parameter values correspond to eutrophic-hypertrophic conditions (European Water Framework Directive, 2000) which promote the development of biofilms on the glass slides.

The first tank (C1) arranged downstream from the generator at a distance of one meter was in hydraulic continuity with the generator; while the second tank (C2) was located downstream from C1 at a distance of 0.20 m from C1 and supplied by a dropwise, ensuring hydraulic discontinuity. The biofilm media were glass slides (76 × 26 mm^2). Twenty slides were placed in tanks C1 and C2 and positioned on supports. C1 tank was of cylindrical shape with a diameter of 0.16 m and a water height of 0.15 m. C2 tank was a rectangular parallelepiped having a width of 0.10 m, a length of 0.30 m and a water height of 0.10 m. Each tank had a volume of 3 L of nutrient solution. The facility had a total storage volume of

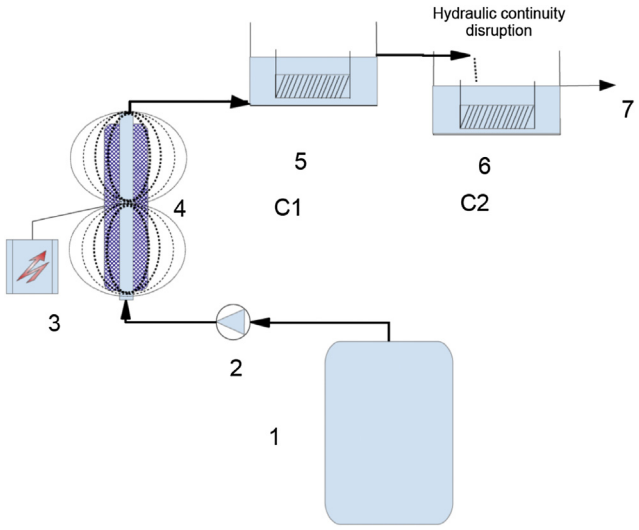

Fig. 1. Schematic representation of one line of the experimental device (1: feeding tank; 2: peristaltic pump; 3 and 4: generator and tube Aqua-4D 60E; 5: tank 1 and glass-slides; 6: tank 2 with glass-slides; 7: outlet).

10.45 L. Hydraulic residence time (volume/influent flowrate) of nutrient solution in a tank was 10.0 ± 1.9 h. The entire setup was placed in the dark in a thermostated room at 20 °C. The bench test consisted of two identical lines arranged in parallel. For the first line the electromagnetic device was active and for the reference line the electromagnetic device was switched off. The electromagnetic device included an electronic control box that generated signals, which were subsequently diffused by the coils inserted into a tube designed to prevent the occurrence of electrical continuity between the coil and the water. Two VLF waves with harmonic frequencies were each generated at a designated frequency on the order of few kHz (confidential data protected by patent: EP2364954A1). The magnitude of the electromagnetic fields was 3.5 mT inside the coils, and 10 V/m and 8 μT close to the external surface of the generator (cf. Section 2.4.2 for measurement method). Due to the long period required for these experiments, they were carried out as a first approach using the settings (frequencies and intensities) recommended by the generator's manufacturer.

Environmental magnetic fields around the experimental device measured in the VLF band were on the order of 1 nT and 0.1 V/m. These values were measured in air with dedicated equipment (Narda EHP50) when the electromagnetic source was switched off according to the method described in Section 2.4.2.

The magnitudes of biofilm exposure to magnetic and electric fields were, respectively, close to 8 nT and 2 V/m. These values were measured in air with dedicated equipment (Narda EHP50) at a distance of 1 m from the electromagnetic source according to the method described in Section 2.4.2.

2.2. Test procedure

The experiment was carried out with three independent trials referred to as test 1, test 2 and test 3. However, there were some differences between the three tests: 1) primarily with regard to the duration of the test, 2) the nature of the inoculum and 3) the number of parameters evaluated for biomass measurement (Table 1). All other experimental conditions were identical. Both lines operated in an open hydraulic circuit. Feeding flow was 208 mL h^{-1}. For this verification approach of the effects of VLF-EMFs on biofilm development, it seemed desirable to test various sources of microorganisms. For test 1 and test 2 the microbial inoculum came from diluted solutions of anaerobic sludge and activated sludge from laboratory reactors. For test 3 the inoculum was taken from the Leysse river (France). Inoculum was added at the beginning of feeding in a proportion of 2 L. Every three to four days one glass slide was removed from each tank and the biofilm was detached by scraping and sonication. The obtained biofilm was quantified using different methods (cf. Section 2.3). The two lines were crossed on the 82nd day for test 1, on the 65th day for test 2 and on the 40th day for test 3: slides from the C1 VLF-EMF line were transferred into the C1 control line and vice versa. The same was done with the slides in C2. The experiment was stopped after 95 days, 80 days, and 63 days for tests 1, 2, and 3, respectively.

2.3. Biofilm measurements

Five different types of measurements of biomass were carried out to quantify the biofilm following normal methods (Merlin and Cottin, 2012). Measurements were made from samples of biofilm detachment solution. The results were expressed per unit area of glass slide. Bacterial density was estimated by measuring the optical density at 600 nm against water as a blank (OD_{600}). COD was measured by the Hach ® micro-method using a Hach DR/5000 spectrophotometer (Hach-Lange, France). A protein assay was performed by the colorimetric bicinchoninic acid method (BCA assay) using the BCA protein assay kit (Pierce, USA) and expressed as bovine serum albumin (BSA) equivalent (Olsen and Markwell, 2007).

An ATP assay was measured by bioluminescence using the TCB™ Kit (TCB-50 Total Control BWWT 50, Aqua-Tools, France). Dosage of exopolysaccharides (EPS) expressed as glucose equivalent was performed by using colorimetry equivalents in the presence of sulfuric acid and warm phenol, as described in Merlin and Cottin (2012).

All measurements were made in triplicate.

2.4. Electrical and electromagnetic measurements

2.4.1. Electric potential

Electric potential measurements for water were performed in the different tanks using a common voltmeter and expressed as a waveform table (Metrix6848, France). The reference was fixed to the grounding circuit of the installation. Discrete representation of the electrical signal in the frequency domain was performed using Fast Fourier Transform (FFT) analysis on 2500 points (Equation (1)).

$$X(k) = \frac{1}{N} \cdot \sum_{n=\frac{N}{2}}^{n=\frac{N}{2}-1} x(n) \cdot \exp\left(-2i\pi \cdot \frac{k}{N} \cdot n \right) \quad \text{for } k \in [0(N-1)] \qquad (1)$$

where: $x(n)$: a sample in the time domain, x (k): a sample in the frequency domain, N: resolution of the FFT, n: time index, k: frequency index.

2.4.2. Electromagnetic field

2.4.2.1. Measurements. Measurements of RF electric and magnetic fields (1–100 kHz) were carried out with dedicated equipment consisting of a three-axis acquisition analyser of RF fields (NARDA EHP-50D; Narda STS, DE). The electromagnetic treatment system was based on two coils (coil 1 and coil 2). Each coil was controlled by a voltage generator at a dedicated frequency corresponding to the term "harmonics". Excitation signals enabled differences (magnitude and phase) between the two control signals to be highlighted and thus the shapes of the magnetic field excitation signals to be visualized. This system did not act as a single coil but as a set of two coupled coils with a global field driven by coil 1 and coil 2.

2.4.2.2. Magnetic field modeling. Electromagnetic modelling of the system allowed the stress, the "beats" generated by the device to be for highlighted. Associating the geometry and the excitation voltage signals of each coil, a physical model was used to determine the magnetic field. The calculus was defined by the Biot-Savart law (Durand, 1968):

Table 1
Differences for operational conditions between the three independent tests conducted.

Test	Duration (days)	Stop VLF-EMF on day	Inoculum	Biomass parameters to quantify biofilm
1	95	82	Anaerobic sludge	COD; bacterial density; BSA; ATP; EPS
2	80	65	Activated sludge	COD; bacterial density; BSA; ATP; EPS
3	63	40	River water	BSA; ATP; EPS

$$\mathbf{B}(\mathbf{r}) = \int \mathbf{G}(\mathbf{r}, \mathbf{r}') \wedge \mathbf{j}(\mathbf{r}') d\mathbf{r}' \quad (2)$$

$$\mathbf{G}(\mathbf{r}, \mathbf{r}') = \frac{\mu_0}{4\pi} \frac{(\mathbf{r}' - \mathbf{r})}{|\mathbf{r}' - \mathbf{r}|^3} \quad (3)$$

where: **B** is the magnetic field (magnetic flux density) at the position **r** from the axes origin, **j** is the current density at the position **r** ′, μ_0 is the permeability of vacuum and **G** is the Green function.

Modeling of EMF was carried out with Flux 2D/3D (CEDRAT, France), an electromagnetic simulation software program. Fig. 2 shows variations and amplitudes of the signal generated by the two coils system at different times.

2.5. Statistical analysis

Statistical analysis was performed using parametric (one-way and two-way ANOVA) or non-parametric (Friedman analysis) tests and the difference between electromagnetic treatment and control was expressed as significant at a significance level of $p < 0.05$. The p value is the estimated probability of rejecting the null hypothesis (hypothesis of "no difference" of the test when that hypothesis is true).

The non-parametric statistical test was carried out when data do not meet criteria for a parametric test (normally distributed, equal variance). Post-hoc tests were conducted in order to decide which groups were significantly different from each other based on F-test for Ryan's test (ANOVA) and based upon the mean rank differences of the groups for Friedman test.

Statistical analyses were performed using the StatEL software (adSciences, France).

3. Biofilm determination

3.1. Experimental results

Three tests were conducted under identical conditions in terms of biofilm exposure to VLF-EMF. Figs. 3 and 4 showing bacterial density and ATP evolution during test 2 illustrate the evolution of biomass parameters of biofilm on glass slides. The evolution of other measured parameters such as COD, protein, and EPS was similar. Table 2 shows values for the five parameters measured on the 60th day of test 2 immediately before the line inversion on the 65th day.

For the different biomass quantification parameters percentages of growth inhibition of biofilm exposed to VLF-EMF versus controls were calculated for the three tests (Table 3). Statistical analysis was performed to compare the different groups of data as described in section 2.5. The results showed inhibition ranging from 42 to 70% for C1-EM tanks. For C2-EM tanks values were much more scattered and ranged from growth activation of 75% to a maximum growth inhibition of 23%.

3.2. Modeling of biofilm growth on glass slides

Two types of growth kinetics were observed according to the conditions of exposure to VLF-EMF and hydraulic continuity (Fig. 3A). The biofilm exposed to electromagnetic waves and in hydraulic continuity grew more slowly than the biofilm control. When hydraulic continuity was not present, the growth of biofilm exposed to the electromagnetic waves was similar to controls. When the biofilm in hydraulic continuity was no longer exposed to VLF-EMF growth has increased again. Based on these observations, we thought it would be possible to describe the biofilm formation on glass slides using a modified Gompertz equation (Zwietering et al., 1990). This type of equation corresponds to growth kinetics of microorganisms regulated by a limiting substrate, such as in a biofilm according to the thickness, and a growth factor independent of biomass (Pavé, 2012). We have assumed that any other phenomenon (e.g. mortality) was negligible when compared to the growth during biofilm formation.

During the phase of biofilm development, several steps may succeed each other (initiation, induction, growth, maturation and detachment), resulting in a sigmoidal growth curve. The different steps can be modeled by Equation (4). The characteristic parameters of sigmoidal growth curve are latency or lag phase (λ), maximum growth rate (k) during the exponential phase, and maximum value (x_{max}) corresponding to the asymptotic value of growth during the stationary phase.

$$x(t) = x_0 + x_{\max} \cdot \exp[b \exp(-k \cdot (t - \lambda))]$$
$$\text{where :} \quad b = \text{constant} \approx \ln\left(\frac{e}{x_{\max}}\right) \quad (4)$$

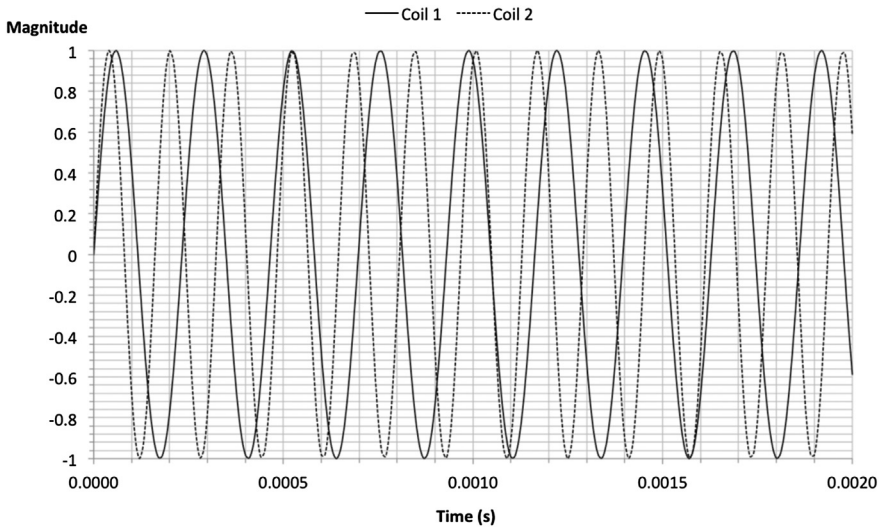

Fig. 2. Simulation of the amplitudes of electromagnetic signals generated by the two coils of the water treatment system versus time.

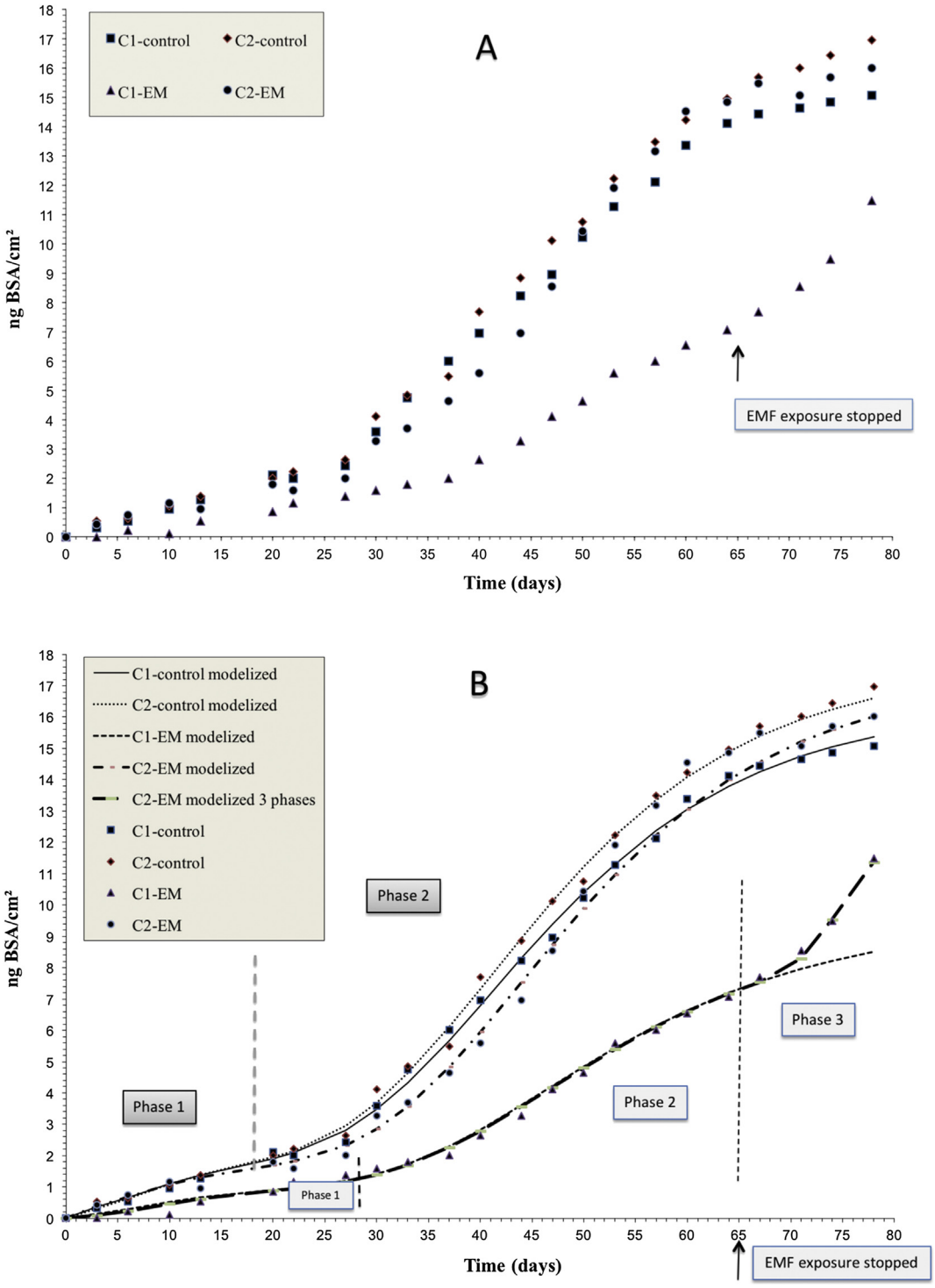

Fig. 3. A. Evolution of protein amount versus time for test 2. B. Fit of modified Gompertz equation. Symbols correspond to experimental data and lines correspond to modeling (Equation 4 or 5) according to phase number.

This model is widely used to characterize bacterial growth kinetics with different conditions. It has the advantage of not being symmetrical relative to the inflection point in contrast to a logistic equation and is therefore more realistic; but it can overestimate the maximum growth rate at times and thus has weak sensitivity.

Biofilm growth was monitored over time by a parameter identified as x_t in our case. This parameter may have been bacterial density, COD, or EPS concentration. In our case the initial value of fixed biomass was zero, i.e. $x_0 = 0$, since only planktonic cells existed at $t = 0$.

It is possible to distinguish the succession of different phases during biofilm development that produces Equation (5) (showing two phases), taking into account iteration with constant values corresponding to each phase:

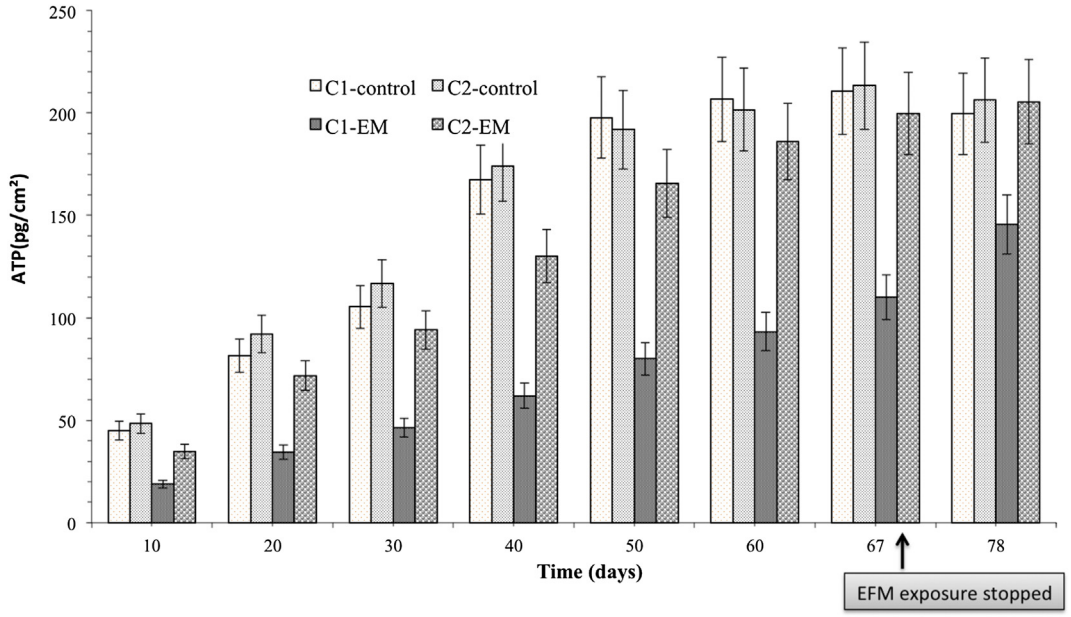

Fig. 4. Evolution of ATP amount versus time for test 2 (mean value of three replicates); error bars represent the uncertainties in the measurements.

Table 2
Values of the different parameters on the 60th day of experiment.

	C1 (control)	C2 (control)	C1 (EM)	C2 (EM)
Bacterial density (cells cm^{-2})	2600	2700	1190	2480
COD (μg cm^{-2})	190	185	92	148
Proteins (μg eq. BSA cm^{-2})	0.0143	0.0142	0.0065	0.0146
ATP (μg cm^{-2})	8.265	8.064	3.732	7.442
EPS (μg eq. glucose cm^{-2})	0.274	0.302	0.168	0.278

C1 tank in hydraulic continuity; C2 tank in hydraulic discontinuity; EM electromagnetic treatment.

Table 3
Inhibition of biomass of biofilm exposed to VLF-EMF expressed in percent of controls (C1-control for C1-EM and C2-control for C2-EM).

	Test	n	C1-EM			C2-EM		
			Mean	SD	p	Mean	SD	p
Proteins (eq. BSA)	1	23	70.37	12.51	$<0.00001^{*F}$	17.79	12.01	$<0.0021^{*F}$
	2	17	57.10	10.24	$<0.00016^{*F}$	11.64	13.80	$<0.9^{F}$
	3	6	42.24	9.19	$<0.00053^{*F}$	−75.30	−34.95	$<0.01^{*F}$
ATP	1	1	63.44	nd	nd	23.64	nd	nd
	2	7	56.68	4.38	$<0.00001^{*A}$	17.54	7.86	$<0.16^{A}$
	3	4	64.10	12.00	$<0.032^{*A}$	15.25	0.50	$<0.26^{A}$
EPS (eq. glucose)	1	1	49.32	nd	nd	−9.44	nd	nd
	2	7	42.67	6.13	$<0.00001^{*A}$	15.45	7.64	$<0.16^{A}$
	3	6	64.80	6.40	$<0.05^{*F}$	4.50	31.25	$<1^{F}$
Bacterial density	1	23	61.49	4.95	$<0.00001^{*F}$	10.43	5.10	$<0.0021^{*F}$
	2	17	56.28	4.57	$<0.00001^{*F}$	1.84	10.95	$<0.38^{F}$
COD	1	23	49.03	7.00	$<0.00001^{*A}$	12.80	8.80	$<0.22^{A}$
	2	17	53.85	5.37	$<0.00001^{*F}$	12.50	8.85	$<0.12^{F}$

n: number of daily measurements, with 3 replicates at each day; SD: standard deviation; p: significance level for statistical test between control and assay using ANOVA (A) or Friedman (F).
*: significant difference at $p < 0.05$.

$$x(t) = x_0 + x_{max1}\cdot\exp[b_1\ \exp(-k_1\cdot(t-\lambda_1))] + (x_{max2}-x_{max1})\cdot\exp[b_2\ \exp(-k_2\cdot(t-\lambda_2))] \quad (5)$$

This type of equation can be useful for modeling a new phase of development when biofilm is no longer exposed to VLF-EMF. Kinetic parameters were estimated according to the modified Gompertz equation using the solver function in the spreadsheet, maximizing the coefficient of determination (r^2) between experimental and modeled values. Experimental data are fitted well regardless of the parameter considered as shown for protein amount in test 2 (Fig. 3B). Until day 65 there were two growth phases: 1) the period of the first phase was 8–20 days depending on measured parameters, and 2) whether biofilm was exposed to electromagnetic waves or not. For C1-EM a new phase of growth was observed when VLF-EMF exposure was stopped.

Table 4 lists all estimated kinetic constants used to plot modeling in the case of bacterial density for the test 2 (Fig. 3B).

Table 4
Kinetic parameters calculated from Equation (4) or (5), case of bacterial density for test 2.

		C1 (control)	C2 (control)	C1 (EM)	C2 (EM)
1st phase	x_{max1} (μg cm^{-2})	1000	850	450	850
	b_1 (−)	2.7	2.7	2.7	2.7
	k_1 (d^{-1})	0.15	0.16	0.16	0.16
	λ_1 (d)	0	0	0	0
2nd phase	x_{max2} (μg cm^{-2})	3950	3850	1750	3700
	b_2 (−)	7.1	7.1	7.1	7.1
	k_2 (d^{-1})	0.0645	0.061	0.061	0.061
	λ_2 (d)	19	16	19	16
3rd phase	x_{max3} (μg cm^{-2})			2500	
	b_3 (−)			7.1	
	k_3 (d^{-1})			0.45	
	λ_3 (d)			67	

C1 tank in hydraulic continuity; C2 tank in hydraulic discontinuity; EM electromagnetic treatment.
Kinetic parameters: latency (λ); maximum growth rate (k); maximum value (x_{max}); mathematical constant (b).

Parameter x_{max}, corresponding to the maximum density of biofilm on glass slides (μg cm^{-2}) appeared to be the most sensitive to the biofilm exposed and in the presence of hydraulic continuity with values of about half of the controls. When VLF-EMF exposure was stopped, the parameter of maximum growth rate increased by a factor 2 relative to the exposure period and compared to controls.

3.3. Discussion

3.3.1. Effect of EMFs in the presence of hydraulic continuity

All the experimental results show that the presence of low EMF limited the biofilm development in C1 when it was in hydraulic continuity with the VLF-EMF generator (Table 3). For all parameters and all tests the average inhibition of biofilm development in tank C1-EM versus C1-control was of the order of 55%: 58.7% ± 8.3% (test 1); 53.3% ± 5.5% (test 2) and 57.1% ± 10.4% (test 3). OD_{600}, COD and proteins are not the most sensitive methods to characterize and quantify cell biomass in biofilm but the results are sufficiently significant to show the reduction of the biofilm biomass with the presence of VLF electromagnetic waves. A certain fraction of the protein, OD_{600} and COD is extracellular and depends on exopolymer production and cellular lysis; but ATP is a direct and interference-free indicator of living biomass. ATP does not accumulate in the biofilm matrix and depends on the growth state of the cell (Lazarova and Manem, 1995). This parameter showed that the active biomass was also reduced by VLF-EMF in the presence of hydraulic continuity. Reduction of the amount of EPS was of the same order of inhibition as other parameters, although EPS can be secreted by the bacteria during stress (Flemming and Wingender, 2010). Uronic acids (components of EPS), acidic amino acids and phosphate-containing nucleotides as negatively charged components of exopolymeric substances can be crucial structural elements of biofilms because they are expected to be involved in electrostatic interactions with multivalent cations (e.g., Ca^{2+}, Mg^{2+} or Fe^{3+}). These cations mediate the formation and/or stabilization of the exopolymeric substances matrix network (Tsuneda et al., 2003). In water treated with electromagnetic fields Ca^{2+} and Mg^{2+} concentrations decrease due to nucleation of ionic calcium or magnesium and their precipitation into calcium or magnesium carbonates (Shahryari and Pakshir, 2008) could influence biofilm growth by acting on the exopolymeric matrix (Trueba et al., 2014). However, no conductivity change was observed between treated and untreated lines in this experiment and ionic strength was approximately 6.2 mM, with 2.4 mM for Ca^{2+} and Mg^{2+}.

To determine persistence of the effect of EM waves on biofilm growth, glass slides were reversed when biofilm growth approached an asymptotic value. A change in slope measured by parameter k_3 was observed (0.45 d^{-1} against 0.061 d^{-1}) indicating a significant increase growth for biofilm on slides previously subjected to electromagnetic waves (C1-EM) and thus disappearance of the bacteriostatic effect. However, applying the electromagnetic waves on glass slides initially positioned in line without excitation (C1-control) did not result in a significant decrease in the rate of biofilm formation during this period. Kinetic constants determined in the C1-control, C2-control and C2-EM tanks had very similar values calculated for the three kinetic parameters, as shown for bacterial density evolution in test 2 (Table 4). The first biofilm development phase corresponds to a period of 8–20 days depending on whether parameters measured and biofilm were exposed to VLF-EMF. These results based on modeling confirm the results of the comparative statistical test (Friedman test), which did not show significant differences between these three experimental conditions ($F_{3,18} = 34.5$; $p < 0.00001$). For the tank in hydraulic continuity with the electromagnetic wave generator (C1-EM), it was primarily the maximum values x_{max} of phases 1 and 2 that were lowest, and they were ~50% lower than values reported for other tanks (Table 4). It was also observed that the latency of phase 2 was longer, extending from two to three days, depending on the parameter measured. On the contrary, growth rates were slightly different. This may correspond to an effect on initiation and induction of biofilm phases, which leads to a lower quantity of microorganisms being able to proliferate in the biofilm. However, it may be that the chosen numerical method for setting the model parameters could be partially the cause of an effect only on x_{max}, which is the most sensitive parameter.

Overall there was a bacteriostatic effect of VLF-type electromagnetic waves which disappeared after emission of these waves was stopped. This was verified after stopping the generator. Then there was a new phase of development modeled according to Equation (5) (phase 3), where biofilm growth was stimulated with a higher maximum rate than in previous phases (Table 4). A decrease in the maximum value of biofilm formation by a factor of approximately 2 was consistently observed in the presence of electromagnetic waves, but not its destruction. Moreover, when electromagnetic waves were stopped, the maximum value was close to the value observed for the controls. Thus, the application of VLF electromagnetic waves of very low intensity has a bacteriostatic, but not a biocide, effect.

3.3.2. Effect of hydraulic discontinuity (C2 tanks)

Nutrient solution flowed between tanks 1 and 2 through a dropwise so that there was no hydraulic continuity. The biofilm development was slightly affected by the presence of electromagnetic waves in the event of a hydraulic discontinuity as in test 1 and 2. For all parameters, average inhibition of biofilm development in tank C2-EM versus C2-control was 11.1% ± 11.2% for test 1 and

11.8% ± 5.4% for test 2. Parametric or non-parametric statistical tests with post hoc analysis were conducted as described in Section 2.5 to compare the effect of VLF-EMF on biomass of biofilm with and without hydraulic continuity between generator and tanks. For inhibition data expressed in percentages versus controls (Table 3), the difference in test score between the hydraulic continuity conditions and hydraulic discontinuity conditions was found to be statistically significant (test 1: $F_{5,22} = 98.71$, $p < 0.00001$; test 2: $F_{5,16} = 68.53$, $p < 0.00001$). However, for rough data, there was a significant difference between C2-EM and C2-control for proteins in test 1 ($F_{3,23} = 52.21$, $p < 0.0021$) and test 3 ($F_{2,5} = 12$, $p < 0.01$), and for bacterial density in test 1 ($F_{3,23} = 52.51$, $p < 0.0021$). Despite some uncertainty concerning the total lack of effect under hydraulic discontinuity conditions; the need for hydraulic continuity for the expression of the VLF-EMF effect is demonstrated by the growth of the biofilm after stopping EMF exposure (Figs. 3A,B and 4). Indeed, the growth rates in tank C2-EM and in the line of tanks without VLF-EMF were very similar. Therefore, it appears that the signal responsible for a bacteriostatic effect was transmitted by water. A distance of approximately 1 m between the tube containing coils and the generator does not explain that the intensity of VLF-EMFs gave rise to the observed effects of ionizing radiation or thermal mechanisms. Electric and magnetic field intensities measured in air were, respectively, lower than 2 V/m and 10 nT at a 1-m distance from the coils (Fig. 5).

The effective isotropically radiated power of the system was only 133 mW; resulting in a root mean square value of 2 V/m as measured in air for the electric field at a distance of one meter.

Taking into account the intensity of this electric field, the specific absorption rate (SAR) in W/kg for exposed biofilm can be established as

$$SAR = \frac{\sigma \cdot E^2}{2 \cdot \rho} \quad (6)$$

where: σ: the electrical conductivity (0.5 S for cellular fluid; Roth, 2000); E: the electric field (V/m); ρ: the biological material density (≈1000 kg/m^3).

With an electric field of 2 V/m the SAR is only 1.10^{-9} W/μg for exposed biofilms. This low value can conventionally explain the lack of an observed effect, or at most a very weak effect, on growth of biofilm exposed without hydraulic continuity. Therefore, "why the need for hydraulic continuity to observe an inhibitory effect?"

3.3.3. Detection of electrical signals and water sensitivity to electromagnetic waves

Within the pilot line, with an active electromagnetic system, a variable electrical potential with a magnitude close to 20 mV was detected in C1-EM placed in hydraulic continuity with the generator (Fig. 6). This signal disappeared while the generator was stopped and was not present in C2-EM in hydraulic discontinuity. Not only did the DC voltage level change during activation of electromagnetic system but also the harmonics of the signal. The frequency analysis provided an analogy with the emitted electromagnetic wave (Fig. 7). Frequencies measured corresponded to the fundamentals (excitation frequencies) and the harmonic components of the electromagnetic system.

Therefore, with hydraulic continuity an electric field appeared to be present in tank C1 (located at a distance of approximately 1 m from the generator). However, according to classical laws of physics, water is should be a diamagnetic substance with a very low sensitivity to magnetic fields. Changing from classical to corpuscular quantum physics does not alter this interpretation because the electromagnetic field in the first quantization is treated according to Maxwell's equations, implying continuous waves and not as quantized photons. Previous literature (Trueba et al., 2014; Cellini et al., 2008; Chua and Yea, 2005; Del re et al., 2004) reveals a sensitivity of living organisms to very weak electromagnetic fields. One has to consider how liquid water would react to a quantized virtual electromagnetic field known to be present in the vacuum generated through H-bonding between water molecules (Bono et al., 2012; Del Guidice et al., 2010).

At the first quantization level, liquid water is adequately described as a flickering tetrahedral H-bonded network of water molecules with a mean residence time for protons ranging from 1 ps at temperature T = 300 K up to 20 ps at T = 250 K (Teixeira

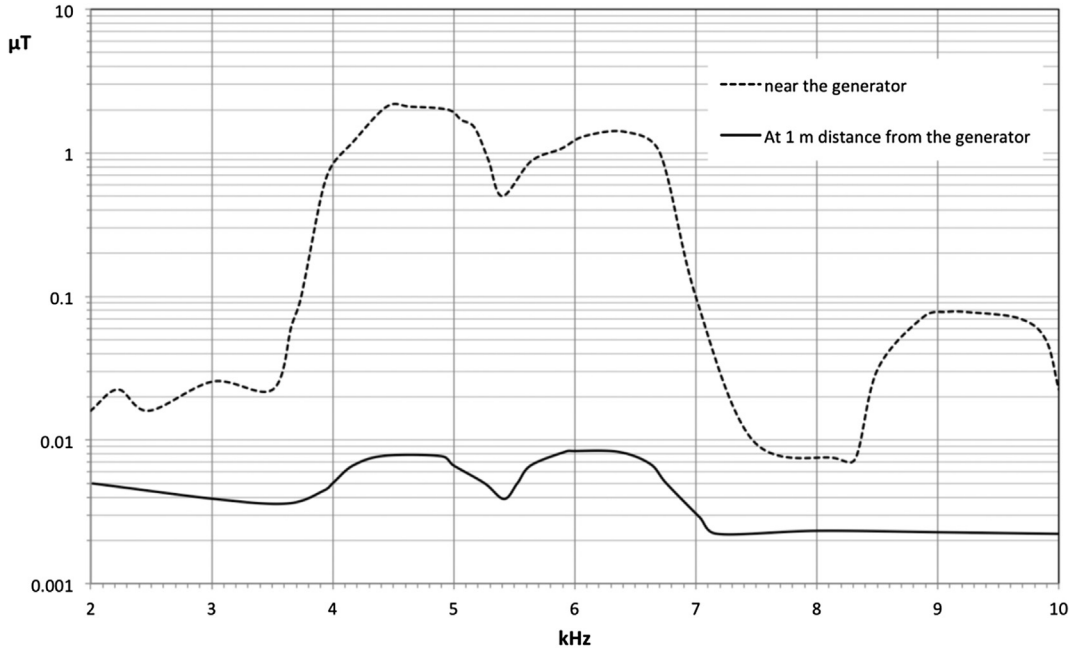

Fig. 5. Intensities of electromagnetic fields measured in the air, near the coils and at a 1-m distance from the generator.

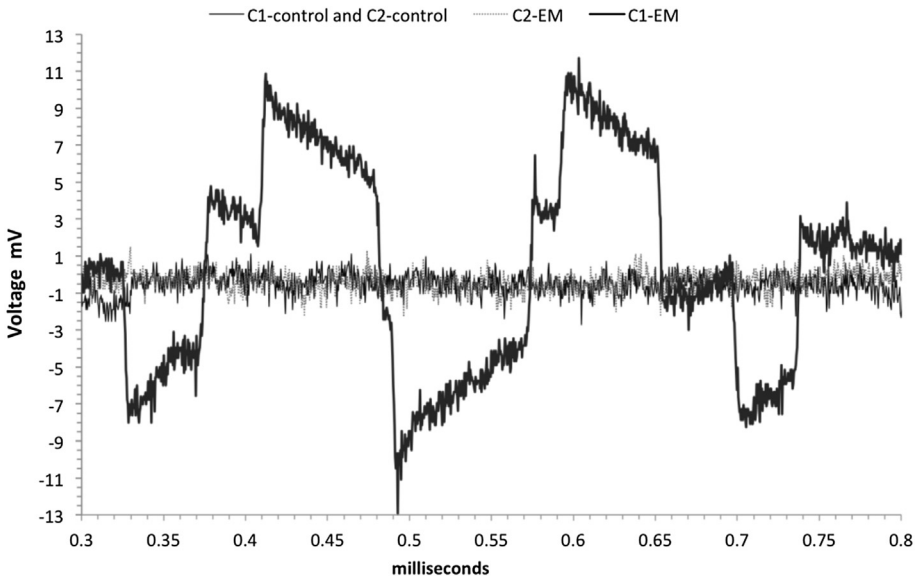

Fig. 6. Time representations of electrical potential measured in water of tanks with and without hydraulic continuity and in water of control tanks.

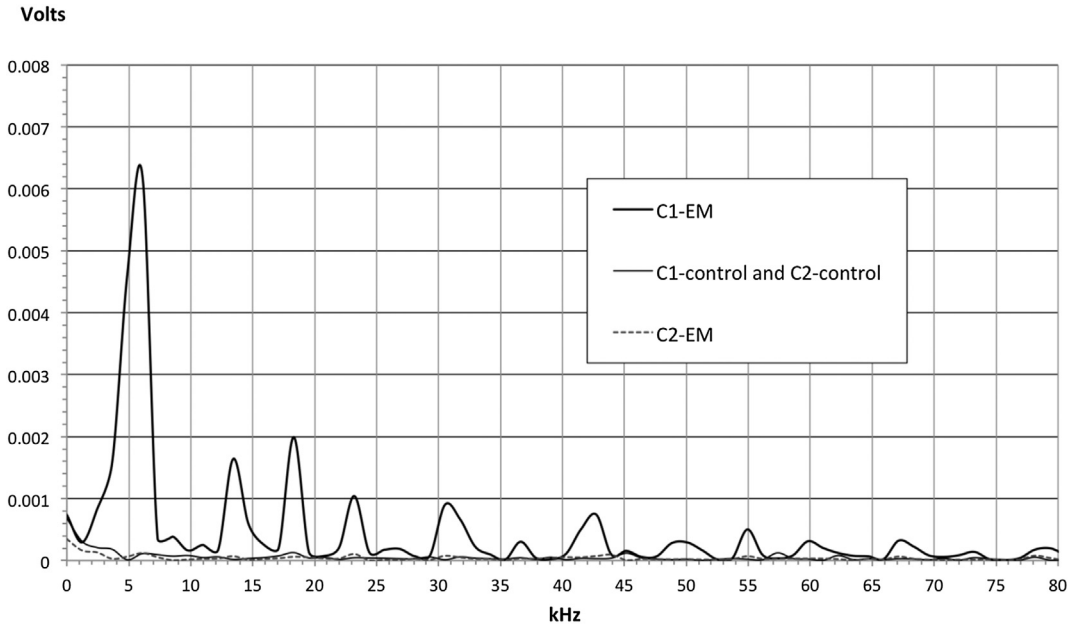

Fig. 7. Frequency representations of electrical potential measured in water of tanks with and without hydraulic continuity and in water of control tanks.

et al., 1985). As the proton is charged its movement should generate a time-dependent current that would generate an electromagnetic field with a frequency of approximately 10^{12} Hz.

It is assumed that due to the incoherent nature of Brownian motion this internal electromagnetic field of liquid water cannot be maintained at a macroscopic scale; this internal electromagnetic field is quickly dampened through destructive interferences over a few H-bonds by the continuous motion of water molecules. According to Quantum Field Theory (QFT) a molecule could be excited by virtual photons emitted from the vacuum; this process is ignored in the first quantization representation. It should be noted that if virtual particles associated with a vacuum fluctuation of energy ΔE cannot be physically detected because they are created and destroyed during a time Δt such that $\Delta E \cdot \Delta t < \hbar$; but they can have measurable effects such as Lamb's shift in the electronic ground state of atoms and Casimir's effect between two metallic plates. Existence of line fields around electrical charges and magnets from the non-zero vacuum impedance ($R \approx 377\ \Omega$) may also produce measurable effects.

In QFT excitation of electrons in molecules could be mediated by virtual photons borrowed from the vacuum, resulting in transient electric currents able to generate transient electromagnetic fields. Consequently, physical properties of liquid water in QFT would be controlled by the entire electronic excitation spectrum of water molecules and not solely by its frontier orbitals energy gap HOMO-LUMO observed in the first quantization. Depending on the total number of molecules N found in a volume V, i.e., depending on matter density N/V, one should observe either phase incoherence between matter fields and virtual electromagnetic fields leading to a gaseous phase, or phase coherence implying condensation in the

form of a liquid or a solid. In QFT a liquid is thus viewed as a collection of coherence domains (CD) having a coherence length controlled by the wavelength of the excited level responsible for the phase locking between matter and macroscopic electromagnetic fields that cannot escape from the CD (Preparata, 2002). Based on a known electronic excitation spectrum of the water molecule of up to 200 eV, it has been shown that emergence of coherence in liquid water was possible through an excited energy level corresponding to a 5 d orbital of the oxygen atom located 12.07 eV above the electronic ground state, creating local electronic currents oscillating with a frequency of $f_r \approx 4 \cdot 10^{13}$ Hz (or 1330 cm^{-1}, corresponding to IR radiations) (Bono et al., 2012; Preparata, 2002). As electrons spend approximately 10% of their time in a diffuse 5 d state localized on oxygen atoms coherent water molecules would have a slightly larger radius (1.5 Å) than incoherent ones (1.1 Å) and are no longer spherical, having two electronic protuberances on the oxygen atom defining a tetrahedron with the two covalent O–H bonds.

The advantage of introducing QFT principles is that the tetrahedral structure of liquid water is thus fittingly explained from first principles. Moreover using this coherent second quantization representation, it was possible to show that at T ≈ 300 K, liquid water should be viewed as a close packing of CD having a radius $R_{CD} = 28.5$ nm separated by an incoherent liquid of higher density having a thickness $2\delta = 18$ nm, corresponding to a coherent/incoherent ratio of 40/60 (Arani et al., 1995). In addition, because the ionization potential of the water molecule is IP = 12.6 eV, it follows that the energy gap for full ionization is only: $\Delta E = 12.6 - 12.07 = 0.53$ eV when the electron spends 10% of its time in an energy level located 12.07 eV above the ground. This is associated with a distance $\Delta r \approx 0.5$ Å for jumping over another water molecule, with a quantum tunneling probability p of 0.91 (Arani et al., 1995). This would mean that approximately 0.10 electrons per water molecule could be in a highly delocalized state and would produce supercurrents owing to their well-defined phase patterns. The large separation of $2\delta \approx 18$ nm between the super-conducting CD obviously prevents liquid water from being a good macroscopic conductor at T = 300 K. However, these freely moving electrons would behave as a charged fluid performing rigid rotations with an angular momentum controlled by the moment of inertia of each CD. This would result in a magnetic moment $\mu = (e \cdot L/2m_e)$ for each CD, which is a QFT explanation of the sensitivity of liquid water to infrared (CD creation) and radio (self-ionization within CD) electromagnetic fields. In fact, loss of coherence in liquid water (only 40% coherence at room temperature) comes from thermal agitation and any decrease in temperature (100% coherence at T = 250 K) or adsorption on any interface increases water coherence. Accordingly, it may be shown that a 70% (weight) of water (or 99 mol%) in a living cell translates to a maximum of 4 layers of water molecules around each biopolymer. Similarly, biofilms are known to be gelified structures made of extracellular polymers having an average molecular weight of 180 kDa (Ras et al., 2011) with a density of approximately 1300 kg m^{-3} (Melo, 2005), and holding approximately 80% (weight) of water. Modeling these polymers of volume $V = 230$ nm^3 as rods of radius R and length L, results in L = 73 nm for R = 1 nm. Adding N water layers having a 0.3-nm thickness results in a hydrated volume $V_n = 229\ (1 + 0.3\ N)^2$ nm^3 (i.e., to a water weight percentage of $\%H_2O = 100(V_n - V)/[230 \cdot 1.3 + (V_n - V)]$). For N = 5 water layers, $V_n = 1433$ nm^3, i.e., $\%H_2O \approx 79\%$. This shows that extracellular water structured by linear polymers as in biofilms should have the same coherence as intracellular water structured by globular polymers. Consequently, 100% coherence for biological interfacial water at T = 310 K can be assumed, for either extracellular (biofilms) or intracellular (cells), with full sensitivity to IR or RF waves at a QFT level of modeling (microscopic scale).

At macroscopic to mesoscopic scales the permittivity, permeability, refractive index and impedance are used to model the response of materials to applied fields through an averaging procedure that works very well when the wavelength is much larger than the size of molecules (Baker-Jarvis and Sung, 2012) and the quasi-static nature of RF-EMF (Habash Riadh, 2006). Assuming an electrical conductivity (σ) of cellular fluid of 0.5 S m^{-1} (Roth, 2000), the magnetic diffusivity (η) defined as $(\mu_o.\sigma)^{-1}$ is equal to 2.22 10^8 m^{-2} s^{-1}, with μ_o, vacuum permeability (4π 10^{-7} H/m). The magnetic field (B) associated with a changing potential difference of 20 mV is approximately 12.5 nT ($=U/\eta$), corresponding to an induced electric current of 9 mA ($=B/\mu_o$). Dividing by q (1.603 10^{-19} C), this electromagnetic strength corresponds to the movement of 6.2 × 10^{16} charges or 1.02 10^{-7} M of H^+ (divided by Avogadro's Number). Next, it is possible to consider the disturbances induced in the biological mechanisms of charge transfer or dielectric responses of biological materials in biofilm exposed to VLF-EMF.

4. Conclusions

Experimental results demonstrate that in water exposed to VLF electromagnetic waves, the formation of biofilm is limited if hydraulic continuity is established between the electromagnetic generator and the biofilm media. The amount of the biofilm biomass measured is approximately two times lower than the control. To optimize the efficiency of this electromagnetic device with VLF at low intensity further studies are currently being conducted to determine the viability of the exposed attached and unattached bacteria (European project, Eurostars “Application of electromagnetic field to biofilm prevention in water distribution systems”). A more complete and complex model should be developed to better quantify the influence of the VLF-EMF on the formation of biofilm exposed.

This process is highly energy-efficient, and physical applications relating to biological phenomena can be numerous. It might be relevant to combine the electromagnetic treatment with an antimicrobial agent to enhance the effects in case of water treatment application.

Many questions remain to explain the observed effect and to understand relationships with the presence of a modulated electromagnetic field in water exposed to VLF electromagnetic waves. Experiments with different frequencies and intensity of VLF waves could also be interesting to investigate in the future to understand their influence.

The application of QFT provides an explanation for the generation of this field in the presence of water. The biofilm is a gelified-type structure containing bound water on its interface with liquid water, making it sensitive to VLF electromagnetic waves. Application of QFT could be used in a future approach to understand the action of waves of VLF on living structures and especially on metabolic mechanisms involving electron transfer and protons but also those involving “hydrophobic interaction,” including adhesion mechanisms. Experiments with bioelectrochemical systems (with electroactive biofilms) are currently being used in our laboratory to investigate the role of VLF-EMF in charge transfers in biofilms.

Acknowledgments

This work has benefited from financial support of the Rhône-Alpes Region (France).

References

Arani, R., Bono, I., del Giudice, E., Preparata, G., 1995. QED coherence and the

thermodynamics of water. Int. J. Mod. Phys. B 9, 1813–1841.
Baker-Jarvis, J., Sung, K., 2012. The interaction of radio-frequency fields with dielectric materials at macroscopic to mesoscopic scales. J. Res. Natl. Inst. Stand. Technol. 117. http://dx.doi.org/10.6028/jres.117.001.
Blank, M., Soo, L., 2001. Electromagnetic acceleration of electron transfer reactions. J. Cell. Biochem. 81, 278–283.
Blenkinsopp, S.A., Khoury, A.E., Costerton, W., 1992. Electrical enhancement of biocide efficacy against pseudomonas aeruginosa biofilms. Appl. Env. Microbiol. 58, 3770–3773.
Bono, E., Del Giudice, L., Gamberale, L., Henry, M., 2012. Emergence of the coherent structure of liquid water. Water 4, 510–532.
Cellini, L., Grande, R., Di Campli, E., Di Bartolomeo, S., Di Giulio, M., Robuffo, I., Trubiani, O., Mariggiò, M.A., 2008. Bacterial response to the exposure of 50 Hz electromagnetic fields. Bioelectromagnetics 29, 302–311.
Chua, L.Y., Yeo, S.H., 2005. Surface bio-magnetism on bacterial cells adhesion and surface proteins secretion. Coll. Surf. B. Biointer. 40, 45–49.
Costerton, J.W., Ellis, B., Lam, K., Johnson, F., Khoury, A.E., 1994. Mechanism of electrical enhancement of efficacy of antibiotics in killing biofilm bacteria. Antimicrob. Agents Chemother. 38, 2803–2810.
Costerton, J.W., Stewart, P.S., Greenberg, E.P., 1999. Bacterial biofilms: a common cause of persistent infections. Science 284, 1318–1327.
Del Guidice, E., Spinetti, P.R., Tedeschi, A., 2010. Water dynamics at the root of metamorphosis in living organisms. Water 2, 566–586.
Del Re, B., Bersani, F., Agostini, C., Mesirea, P., Giogi, G., 2004. Various effects on transposition activity and survival of Escherichia Coli cells due to different ELF-MF signals. Radiat. Environ. Biophys. 43, 167–193.
Di Campli, E., Di Bartolomeo, S., Grande, R., Di Giulo, M., Cellini, L., 2010. Effects of extremely low-frequency electromagnetic fields on Helicobacter pylori biofilm. Curr. Microbiol. 60, 412–418.
Durand, E., 1968. Tome Magnétostatique, Edition MASSON. France, Paris.
European Communities (EC), 22 December 2000. Directive 2000/60/EC of the European Parliament and of the Council of the 23 October 2000 establishing a framework for community action in the field of water policy. Off. J. Eur. Commun. Off. J. L 327, 22/12/2000 P. 0001-0073. http://eur-lex.europa.eu/LexUriServ/LexUriServ.do?uri=OJ: L:2000:327:0001:0072:.
Flemming, H.C., Wingender, J., 2010. The biofilm matrix. Nat. Rev. Microbiol. 8, 623–633.
Habash Riadh, W.Y., 2006. Biological effects of electromagnetic fields. In: Bansal, Rajeev (Ed.), Engineering Electromagnetics Applications. CRC Taylor and Francis, Boca Raton, FL, pp. 189–210.
Jefferson, K.K., 2004. What drives bacteria to produce a biofilm. Fems Microbiol. Lett. 236, 163–173.
Lazarova, V., Manem, J., 1995. Biofilm characterization and activity analysis in water and wastewater treatment. Water Res. 29, 2225–2247.
Marchettini, N., Del Giudice, E., Voeikov, V., Tiezzi, E., 2010. Water: a medium where dissipative structures are produced by a coherent dynamics. J. Theor. Biol. 265, 511–516.
Melo, L.F., 2005. Biofilm physical structure, internal diffusivity and tortuosity. Water Sci. Technol. 52, 77–84.
Merlin, G., Cottin, N., 2012. Lab-scale performance evaluation of vertical flow reed beds for the treatment of chlorobenzene contaminated groundwater. J. Environ. Prot. 3, 847–855.
Mueller, R.F., 1996. Bacterial transport and colonization in low nutrient environments. Water Res. 30, 2681–2690.
O'Toole, G., Kaplan, H.B., Kolter, R., 2000. Biofilm formation as microbial development. Annu. Rev. Microbiol. 54, 49–79.
Olsen, B.J., Markwell, J., 2007. Assays for the determination of protein concentration. Curr. Protoc. Protein Sci. 4–17.
Pavé, A., 2012. Chapter 3 Growth Models – Population Dynamics and Genetics, in Modeling Living Systems: from Cell to Ecosystem. John Wiley & Sons, Inc, Hoboken, NJ, USA.
Pickering, S.A.W., Bayston, R., Scammell, B.E., 2003. Electromagnetic augmentation of antibiotic efficacy in infection of orthopaedic implants. Bone Jt. Surg. 85B, 588–593.
Preparata, G., 2002. An Introduction to Realistic Quantum Physics. World Scientific, New Jersey.
Ras, M., Lefebvre, D., Derlon, N., Paul, E., Girbal-Neuhauser, E., 2011. Extracellular polymeric substances diversity of biofilms grown under contrasted environmental conditions. Water Res. 45, 1529–1538.
Roth, B.J., 2000. In: Bronzino, Joseph D. (Ed.), The Electrical Conductivity of Tissues. The Biomedical Engineering Handbook, second ed. CRC Press LLC, , Boca Raton.
Shahryari, A., Pakshir, M., 2008. Influence of a modulated electromagnetic field on fouling in a double-pipe heat exchanger. J. Mater. Process Technol. 203, 389–395.
Teixeira, J., Bellissent-Funel, M.C., Chen, S.H., Dianoux, A.J., 1985. Experimental determination of the nature of diffusive motions of water molecules at low temperatures. Phys. Rev. A 31, 1913–1917.
Trueba, A., Garcia, S., Otero, F.M., 2014. Mitigation of biofouling using electromagnetic fields in tubular heat exchangers-condensers cooled by seawater. Biofouling 30, 95–103.
Tsuneda, S., Aikawa, H., Hayashi, H., Yuasa, A., Hirata, A., 2003. Extracellular polymeric substances responsible for bacterial adhesion onto solid surface. FEMS Microbiol. Lett. 223, 287–292.
Zhou, S.A., Uesaka, M., 2006. Bioelectrodynamics in living organisms. Int. J. Eng. Sci. 44, 67–92.
Zwietering, M.H., Jongerburger, I., Rombouts, F.M., Van't Riet, K., 1990. Modeling of the bacterial growth curve. Appl. Env. Microbiol. 56, 1875–1881.